Relazione interna OGS 2024/18

OGS National Institute of Oceanography and Applied Geophysics

Some considerations on background noise and detection capability of the "San Potito-Cotignola seismic monitoring network"

January 2024

Authors:
Eduardo Diez, Denis Sandron, Adelaide Romano, Mariangela Guidarelli, Marco Romanelli, Fabio Franceschinel

Director:
Prof. Matteo Picozzi

Index

1. INTRODUCTION

To evaluate the quality of a seismic network, one of the most important parameters is "detection", which indicates the minimum value of magnitude that can be detected by the network at a given point in space, depending on its geometry and density, as well as the background noise at each station.

Estimating the detection capability of a seismic network is extremely important both for planning a new network and for evaluating the performance of an existing network and determining areas for improvement. Some of the possible motivations for implementing and performing such a task include consistent and uniform detection of seismicity over the entire target monitoring area, evaluation of the network design and the possible changes that can be made to it to achieve a target value for the completeness of the resulting seismic catalog, and continuous monitoring of the network's operability and efficiency by measuring the acquired data and its overall performance.

An important concept is that detection capability is a property that is neither spatially uniform nor constant over time. There are several reasons for this, such as the functionality of the instruments, the quality of the overall hardware, which can vary from station to station and deteriorate over time, atmospheric conditions, anthropogenic noise and local soil conditions. All these factors affect the noise level of the recorded signal.

Continuous monitoring of the quality of a station makes it possible to estimate the quality of the seismic network at a given time or in a given time interval. Estimating how much and where the seismic network can detect seismicity and storing this information in a database is useful for studying the characteristics and variability of the parameters contained in the data recorded by the network itself.

These aspects are particularly important for very sensitive networks capable of recording microseismicity down to the background.

In this report, we determine the coverage of the San Potito-Cotignola seismic monitoring network (SPCSN) by using the empirically estimated spectral level of seismic noise at each station and some theoretical relationships to predict the signal amplitude of a seismic event at individual stations. We will estimate the distribution of the smallest locally detectable magnitude and evaluate the number of triggered stations for a reference magnitude.

2. SAN POTITO-COTIGNOLA SEISMIC MONITORING NETWORK

The San Potito-Cotignola Seismic Monitoring Network (SPCMN), also called SP network, consists of fifteen seismic stations with permanent geodetic GNSS stations that contribute to the integrated microseismic and geodetic network of the San

Potito and Cotignola gas storage concession operated by Edison Stoccaggio Spa (Figure 1).

The stations of the network are equipped with both borehole and surface instruments to reduce the influence of anthropogenic noise, which mainly propagates in the superficial layers of the ground. In order to cover the entire dynamic range of seismic signals, the stations are also supplemented with strong motion instruments to record larger magnitude earthquakes. Table 1 shows the location of the stations of the SP seismic network and the installed instruments.

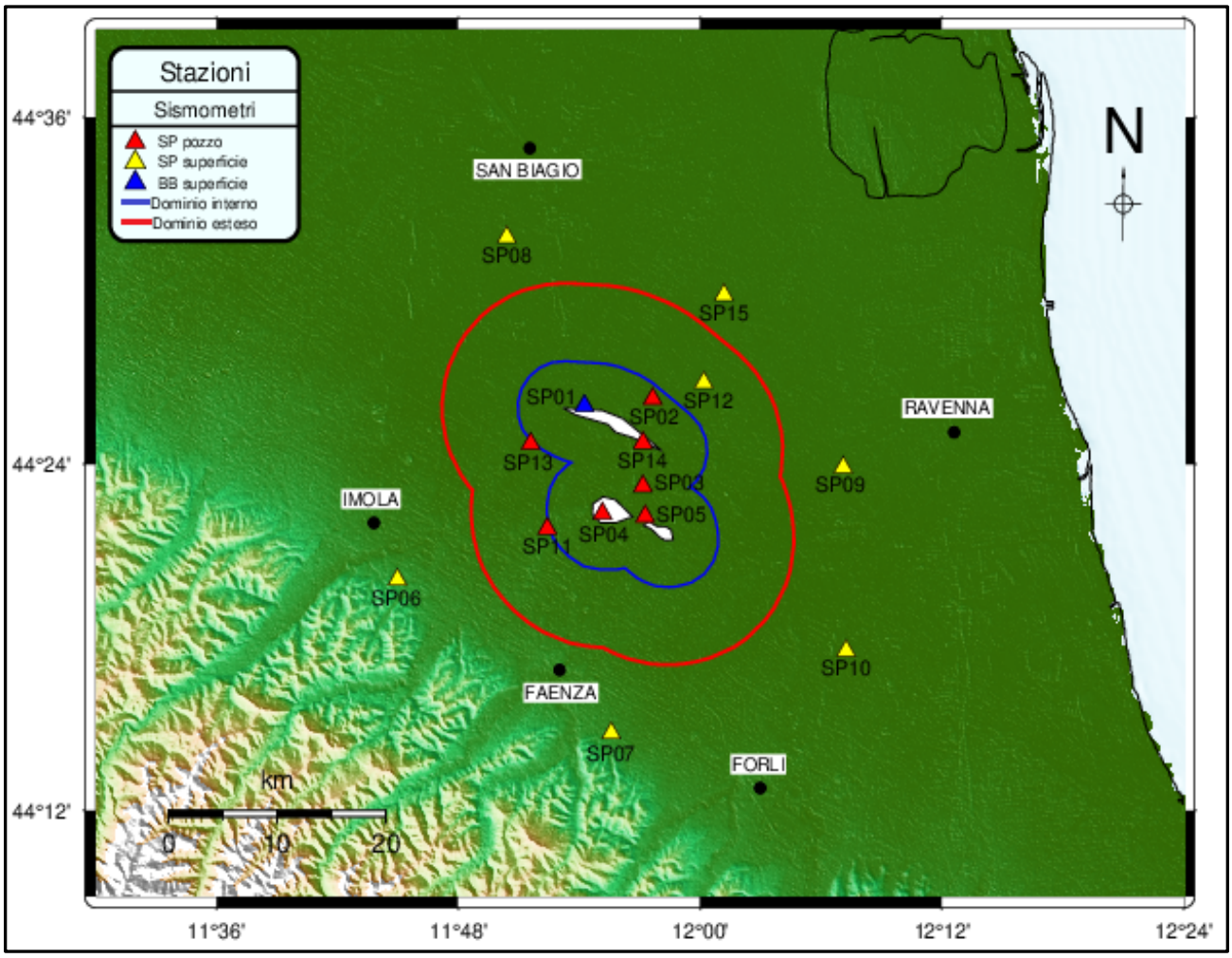

Figure 1. Areas interested in the seismic monitoring of the "San Potito and Cotignola Stoccaggio" natural gas storage facilities (white polygons) by the SP network. The red triangles represent the stations with borehole seismometers, while the yellow triangles are stations with surface sensors. The blue and red polygons represent two reference areas corresponding to the coverage areas indicated by the ILG of MiSE (MiSE-UNMIG, 2014). The inner domain (ID) surrounds the reservoir up to a distance of 3 km, and the extended domain (ED) extends up to 15 km from the outer edge of the reservoir area.

The seismic network consists of two groups of stations:

- an internal core consisting of 7 stations with short-period borehole sensors (SP02, SP03, SP04, SP05, SP11, SP13 and SP14) surrounding the storage area. In addition, station SP01 is equipped with a broadband seismometer. These stations cover the area around the reservoir and are mainly intended to detect microseismicity possibly caused by the storage activities.

- an external group consisting of 7 stations (SP06, SP07, SP08, SP09, SP10, SP12 and SP15) located at various distances between 10 and 20 km from the central core. These stations are placed to cover the area where the induced seismicity parameters are to be recorded with higher accuracy.

Table 1. List of stations of the network "San Potito and Cotignola" (SP) with: Station code (Sta_Id); data logger type; instrument type (seismometer, SS and accelerometer, SA serial numbers); geographical parameters (Lat, Lon, depth, altitude); date of start of operation.

Stat_Id	Datalogger	Sensors	Latitude (N)	Longitude (E)	Depth (m)	Elevation (m)	Date on
SP01	SARA SL06-BB	SS08(2233)	44.433748	11.904231	0.5	10	17/12/2018
		---			---		
SP02	SOLGEO DYMAS 24	SS10BH(2637)	44.437697	11.960797		7	10/10/2018
		SA10(2647)			0.5		
SP03	SOLGEO DYMAS 24	SS10BH(2642)	44.387289	11.952630		14	09/10/2018
		SA10(2648)			0.5		
SP04	SOLGEO DYMAS 24	SS10BH(2638)	44.371509	11.919130		17	27/09/2018
		SA10(2645)			0.5		
SP05	SOLGEO DYMAS 24	SS10BH(2639)	44.369958	11.954506		14	27/09/2018
		SA10(2646)			0.5		
SP06	SOLGEO DYMAS 24	SS02(2635)	44.333389	11.749564	0.5	66	23/10/2018
		SA10(2649)			0.5		
SP07	SOLGEO DYMAS 24	SS02(2636)	44.244694	11.926417	0.5	48	20/11/2018
		SA10(2650)			0.5		
SP08	SOLGEO DYMAS 24	SS02(2632)	44.530917	11.840028	0.5	3	24/09/2018
		SA10(1070)			0.5		
SP09	SOLGEO DYMAS 24	SS02(1642)	44.398181	12.118394	0.5	1	24/10/2018
		SA10(2742)			0.5		
SP10	SOLGEO DYMAS 24	SS02(2634)	44.398181	12.120789	0.5	10	21/11/2018
		SA10(2743)			0.5		
SP11	SOLGEO DYMAS 24	SS10BH(2643)	44.362811	11.873497		24	12/10/2018
		SA10(2651)			0.5		
SP12	SOLGEO DYMAS 24	SS02(2630)	44.447058	12.003094	0.5	3	27/09/2018
		SA10(2628)			0.5		
SP13	SOLGEO DYMAS 24	SS10BH(2640)	44.411881	11.859742		14	25/10/2018
		SA10(2744)			0.5		
SP14	SOLGEO DYMAS 24	SS10BH(2170)	44.407844	11.945058		13	21/11/2018
		SA10(2745)			0.5		
SP15	SOLGEO DYMAS 24	SS02(2633)	44.497611	12.019667	0.5	5	25/09/2018
		SA10(2629)			0.5		

The stations are equipped with professional instruments from SARA electronic instruments s.r.l. and SOLGEO. Specifically, the sensors are the SARA SS08 broadband seismometer, the SARA SS02 short-term surface seismometer and the SARA SS10BH borehole seismometer (https://www.sara.pg.it/).

In order to cover the entire dynamic range and utilise the capabilities of the data loggers, SARA SA10 accelerometers were also installed to record strong earthquakes where the signal obtained from the velocimetric seismometers could be saturated in amplitude. It is a force-balance feedback type instrument with a flat response to ground acceleration from DC to 100 Hz and a stable phase response within this passband.

The digitizers are SOLGEO DYMAS24 and SARA SL06, advanced "smart" multi-channel and 24-bit digitizers for seismic measurements. Their main features are their robustness, low power consumption and compatibility with SeedLink protocols and MiniSeed and other formats (https://www.solgeo.it).

Figure 2 shows the instruments used to set up the recording channels in the SP network stations.

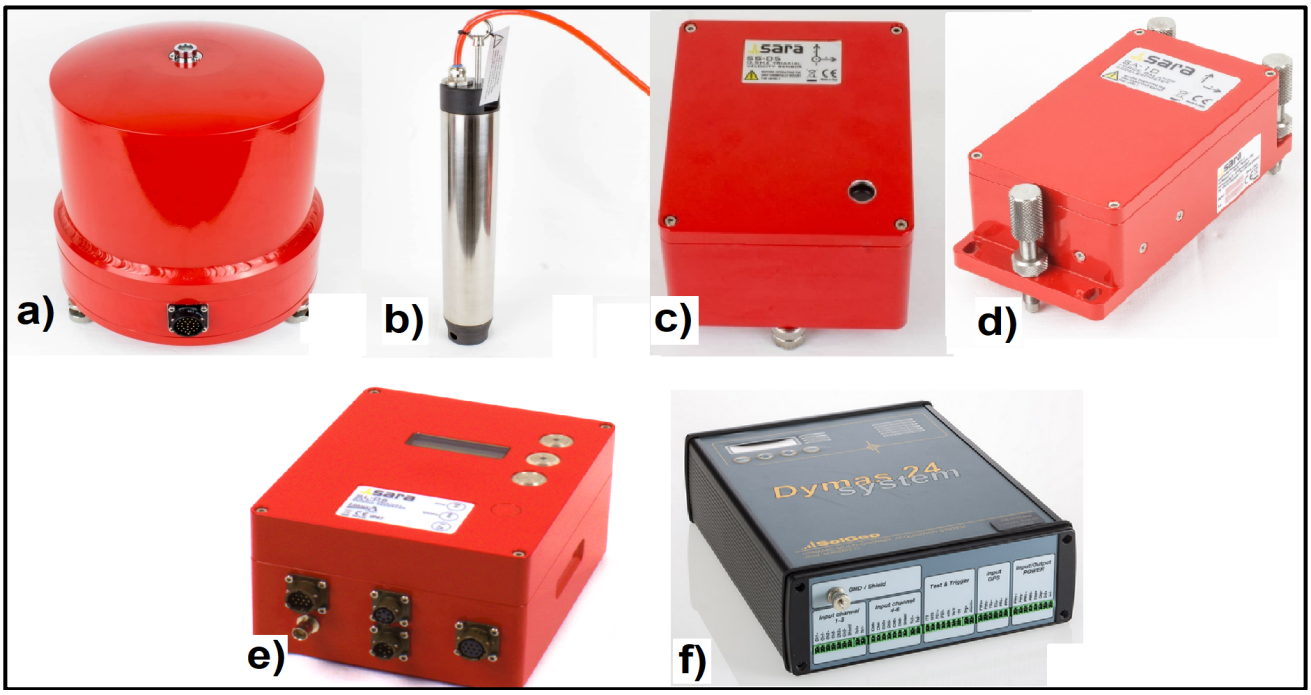

Figure 2. Photos of the instruments installed in the SP network: a) SARA SS08 broadband seismometer; b) SARA SS10BH short-period borehole seismometer; c) SARA SS02 short-period surface seismometer; d) SARA SA10 force-balance accelerometer; e) SARA SL06 digitizer; f) SOLGEO DYMAS24 digitizer.

The borehole sensors were equipped with a coupling system developed by SARA, which consists of a steel blade that is tensioned by two flanges integrated into the sensor (Figure 2b). The tension of the blade is adjusted so that the sensor can slide into the pipe with a suitable weight. Once at the bottom of the borehole, the weight is then removed from above.

3. NOISE

Every seismic sensor in operation records background noise everywhere, which can be defined as the part of the continuous signal that cannot be properly associated with an earthquake. This unavoidable interference can be of instrumental origin and come from the same equipment that makes it up, of electromagnetic origin due to the poor shielding of the components, or of anthropic origin for the activities that take place in the vicinity of the recording site (industry, agriculture, vehicle traffic, household appliances) and of natural origin for both direct (wind, rain) or indirect (sea storms, rivers) phenomena.

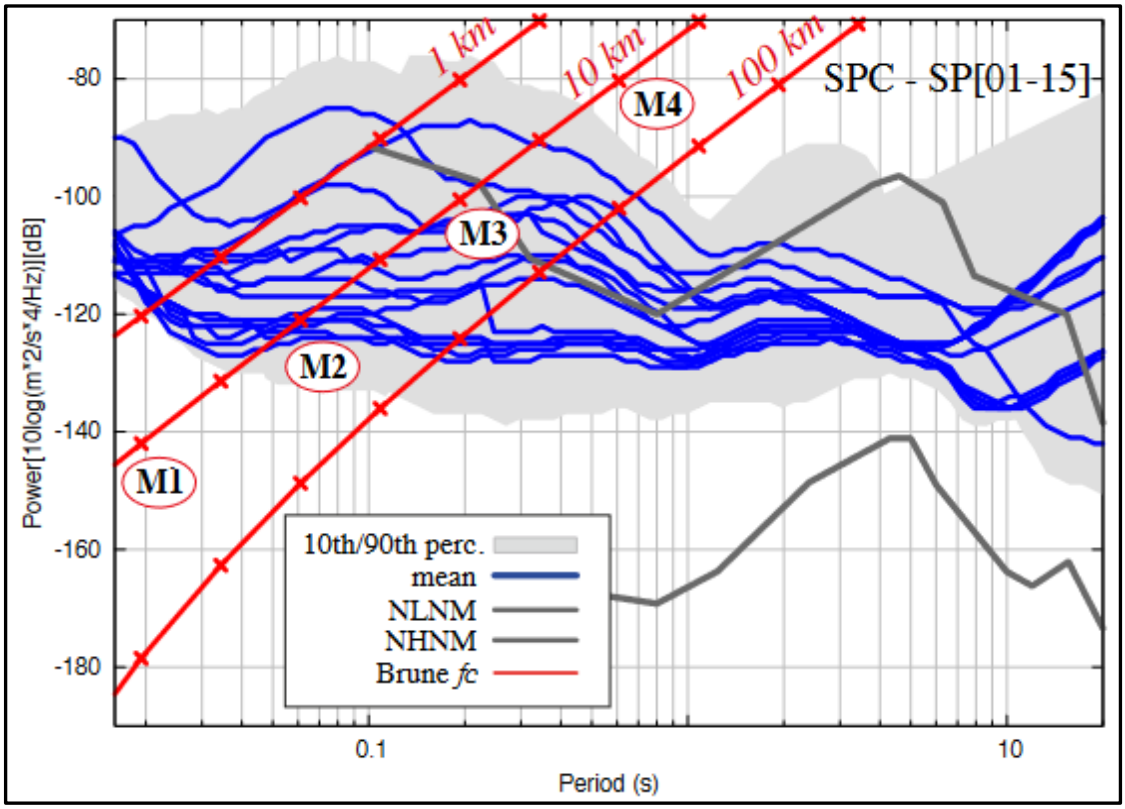

Figure 3. The "mean" noise levels of the stations of the SP network (blue lines) on a vertical component broadband channel (HHZ) after one month of continuous recording (July, 2022). The standard reference curves "New High Noise Model" (NHNM) and "New Low Noise Model" (NLNM) are shown in dark grey (Peterson, 1993). The red lines show corner frequencies and P-wave amplitudes (Brune, 1970) for earthquakes of magnitudes [M1-M3] and distances [1, 10, 100 km].

A complete description of the noise characteristics of a seismic station requires the acquisition and processing of signals over long time intervals, preferably continuously.

In this study, we have used both the waveform recordings and the seismic events obtained from the SP network during one month of operation (July, 2022).

In particular, the data are processed using PQLX, an open-source software package distributed by IRIS (2017) to evaluate the performance of the network's seismic station and the quality of the recorded data (McNamara & Boaz, 2005 and 2010). It calculates the power spectral density (PSD) and probability density function (PDF) from the full waveform by processing multiple trace segments with a predefined time length and overlap, respectively. The PSDs are stored in a MySQL database, which allows access to a specific series of PSDs via a user interface.

From the PDF of a channel, the variables corresponding to the most probable disturbance level (i.e. "mode", "mean", "median" and the levels corresponding to the percentiles of the probability curve (5 and 95%)) can be extracted.

The data corresponding to the "mean" noise levels of the stations of the SP network, related to one month of continuous recording (July, 2022) on a vertical component broadband and short-term channel (HHZ and EHZ), are shown in Figure 3 and compared with the standard reference curves "New High Noise Model" (NHNM) and "New Low Noise Model" (NLNM) (dark gray lines) of Peterson (1993).

The individual diagrams of the individual stations of the SP network are shown in Appendix 1.

From the point of view of seismic noise and its distribution in the time domain, even if all stations show a behavior within the optimal range and a homogeneous trend between them, the SP network can be considered with high noise levels in certain period bands.

Analyzing the PSD curves of the 15 stations in detail, it is observed that in the period band between 0.06 and 0.3 seconds (where the signals corresponding to low energy local earthquakes are expected), the PSD value is generally between -80 dB and -112 dB. However, the noise behavior varies considerably at each station, depending on the local conditions, i.e. the type of sensor installation and the local antrophogenic noise. Even with the same borehole or surface sensors, there are significant differences between the values obtained.

For example, station SP01, which is equipped with a different sensor (broadband seismometer SARA SS08), shows a high PSD value above Peterson's NLNM model in the band used. This could be due to the high sensitivity of this sensor, which is three times higher than that of the SS02 and SS10BH seismometers, and also to the poor isolation from external noise sources (see Figure 4).

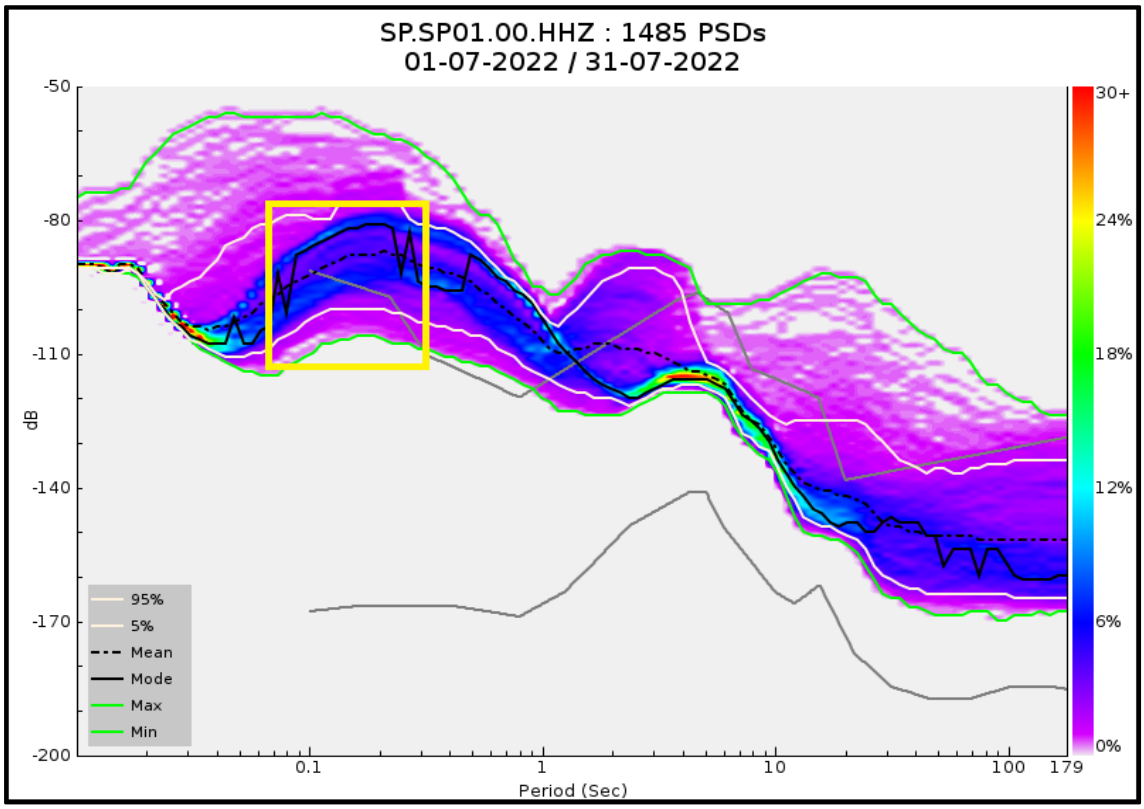

Figure 4. Probability density functions resulting from the analysis of the continuous seismic noise recording for the SP01 station (broadband). The yellow box indicates the period band used in the study where a high noise level was observed, approximately -80dB|-90dB of PSD values for the statistical mean and mode values (dashed and solid black lines, respectively). The gray lines represent the low and high noise reference models (Peterson, 1993). The other lines represent the other statistical parameters, namely the 5th and 95% percentiles (solid white lines) and the maximum and minimum values (two solid green lines).

In the case of the borehole seismometers, Figure 5a and 5b show the PSD plots for stations SP03 and SP05, which show the above-mentioned local noise variations for similar instruments installed in the same way. Here the observed difference between the best and the worst case is about 40 dB.

The same applies to seismometers installed on the surface, i.e. the noise curves to be expected from these instruments are not homogeneous and depend strongly on local conditions. Although, according to Bormann (2002), cultural noise decreases rapidly at depth, we see stations installed at the surface with a lower noise level, at least in the period (frequency) band used in this study, than their similar stations installed in boreholes and vice versa.

This demonstrates a strong correlation between the PSD values and their dependence on local conditions. Figure 6 illustrates the principle explained above and shows that it is possible to detect significant differences between two stations with similar instrumentation. In this case, the PSD diagrams of stations SP07 and SP10 (surface installation) are compared and show a deviation of about 30 dB.

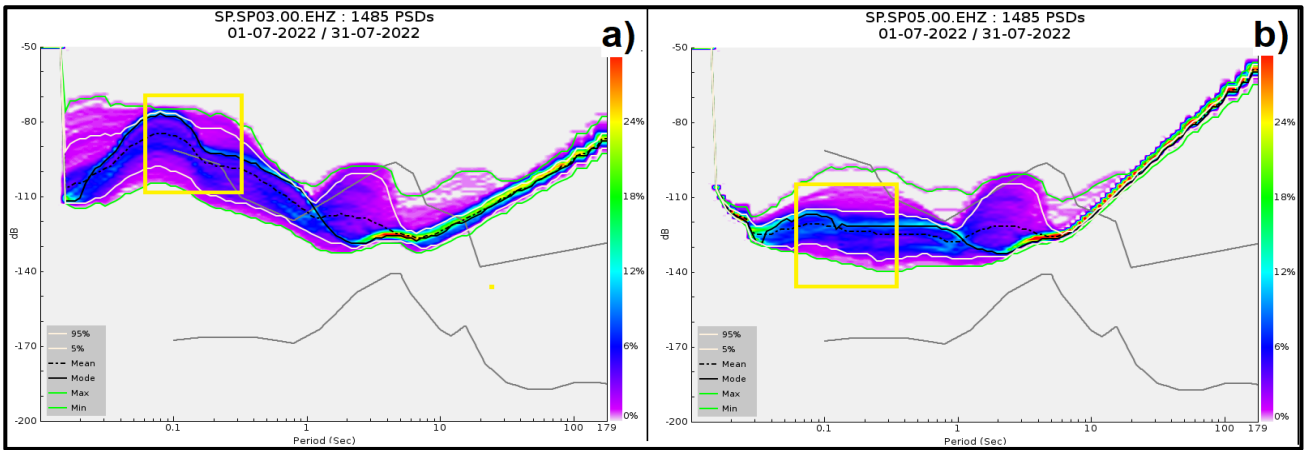

Figure 5. Comparison between the probability density functions resulting from the analysis of the continuous seismic noise recordings for the two different borehole stations: (a) Station SP03, which has the highest seismic noise level and represents the worst case; (b) Station SP05, which is an example of the lowest seismic noise level. The yellow box indicates the period band used in the study, where a difference of about 40 dB can be observed between the PSD values for the statistical mean and mode values (dashed and solid black lines, respectively) between the two stations. The gray lines represent the low and high noise reference models (Peterson, 1993). The other lines represent the other statistical parameters, namely the 5th and 95% percentiles (solid white lines) and the maximum and minimum values (two solid green lines).

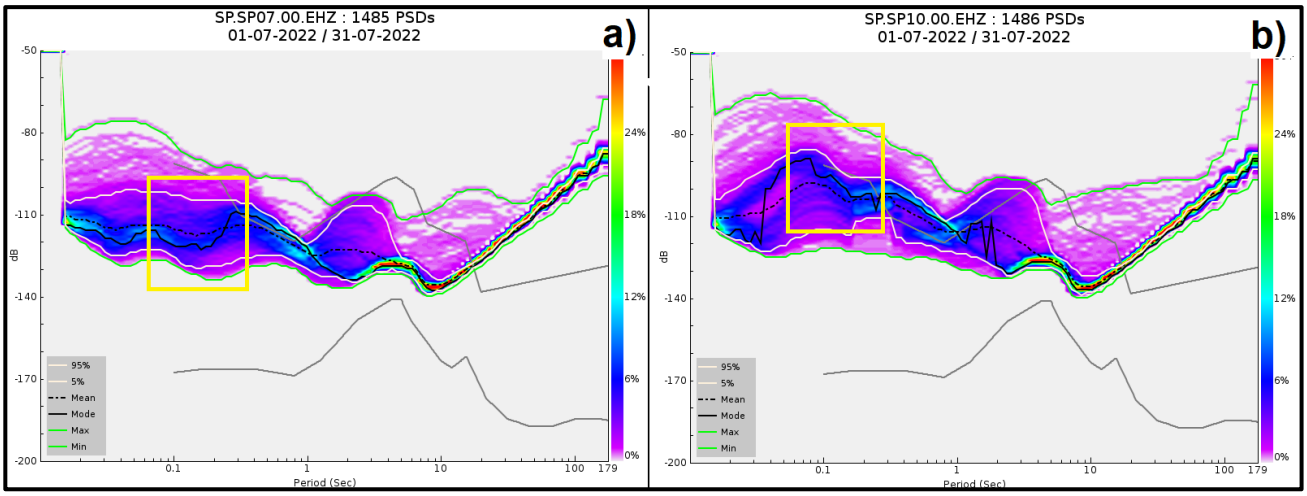

Figure 6. Comparison between the probability density functions resulting from the analysis of the continuous seismic noise recordings for the two different surface stations: (a) Station SP07, which is an example of the lowest seismic noise level; (b) Station SP10, which is an example of the highest seismic noise level. The yellow box indicates the period band used in the study, where a difference of about 30 dB can be observed between the PSD values for the statistical mean and mode values (dashed and solid black lines, respectively) between the two stations. The gray lines represent the low and high noise reference models (Peterson, 1993). The other lines represent the other statistical parameters, namely the 5th and 95% percentiles (solid white lines) and the maximum and minimum values (two solid green lines).

To summarize, the noise values at the 15 stations vary and depend mainly on the local conditions and less on the type of installation. However, it should be noted that our study is only based on a one-month time series (July 202)2 and it is therefore very difficult to estimate the variations in noise during a whole year and in different seasons.

These very different noise levels at the individual stations determine the detection threshold of the entire SP network, which is shown in the following sections of this document.

4. MAGNITUDE EARTHQUAKE THEORETICAL DETECTION THRESHOLD

4.1.1 Method

The approach of Marzorati and Cattaneo (2016) assumes that both the earthquake source and the propagation path can be theoretically described by the Brune spectrum (Brune, 1970) or a suitable spectral attenuation law, then the seismic noise at each station is the fundamental observable, which can be expressed as power spectral density (PSD) according to McNamara and Boaz (2005). Since we can theoretically calculate the signal at each station for a given earthquake, the seismic noise directly affects the observed signal-to-noise ratio (SNR) and influences the detection threshold at each site.

For the SPCMN, the magnitude is calculated using the attenuation law developed by Bragato and Tento (2005), a relationship based on a large data set of observations from north-eastern Italy. Compared to Richter's original formula, it is characterized by a stronger attenuation of the amplitudes at a distance of less than 100 km and is better suited to represent the attenuation by the valley sediments for the SP stations. In addition, as Hutton and Boore (1987) have shown, the formula is calibrated for the hypocentric distance of 17 km instead of the 100 km of the original formula, a distance that is much more suitable for estimating the magnitude of local earthquakes.

The calculation formula used is therefore as follows:

$$M_L = \log_{10}(A) + 2.230(D) - 0.0039(D) - 3.7519 \qquad (1)$$

On the other hand, the mean (rms) noise amplitude at each station is calculated independently in the form of a PSD function; this is done using the PASSCAL Quick Look eXtended (PQLX) program (McNamara and Boaz, 2005).

To convert the PSD into a corresponding waveform amplitude defined in the time domain, we follow the approach proposed by Aki and Richards (1980) and Bormann (2002).

Essentially, this approach assumes that for a given frequency band, the maximum amplitude of a wave $f(t)$ near t = 0 can be approximately determined by

the product of the so-called energy spectral density with the waveband width. In this study, a frequency band between 3 Hz and 15 Hz was used, which corresponds to the filter used in picking (see yellow boxes in Figures 4, 5 and 6).

Assuming that the seismic noise is a stationary stochastic signal (it has finite power), and using the Fourier transform property (Parseval's theorem), we can express the noise amplitude, which is usually written as the RMS value of the signal, in the form:

$$A_{rms} = \sqrt{2P(f_2 - f_1)} \qquad (2)$$

Where P is the signal power and is obtained by integrating the PSD over the frequency band $(f_2 - f_1)$.

Finally, the three-dimensional space is discretized into an arbitrary number of parallel planes in depth and with a regular mesh of points for the grid search. In the calculation, each grid point represents the hypocenter of a local magnitude earthquake in a predefined area. The earthquake with the lowest detectable magnitude is selected and the corresponding value is linked to the analyzed hypocenter. The union of all hypocenters with an associated threshold magnitude forms the detection map.

The geographical area considered in this study lies between 44.00° and 45.00° north latitude and 11.00° to 12.00° east longitude and corresponds to the effective coverage area of the SPCMN network, which is designed for the detection of local earthquakes.

The objective is the minimum detection magnitude, i.e. the smallest magnitude that can be detected in a given time interval and a given "operational state" of the seismic network (i.e. magnitude to be detected, number of stations required to report an earthquake, SNR ratio corresponding to the percentage of stations in operation, etc.), given the noise level at each station and the number of stations where the a priori defined signal-to-noise ratio (SNR) is exceeded. In this way, an estimate is made of the amplitude that would be recorded by a seismic station according to the magnitude-distance pair. If several neighboring stations meet the condition of exceeding the specified SNR threshold, this earthquake is declared as recorded by the network.

To summarize, the method proposes to use the signal-to-noise ratio, which is the quotient between the amplitudes of two signals, one of which (the dividend) is obtained by applying the local magnitude law developed by Bragato-Trento, while the other (the divisor) is obtained from the power spectral density (PSD) functions using the approach of Aki and Richards (1980).

4.1.2. Results and discussion

We performed some synthetic tests for the SPCMN network (Figure 7). Specifically, starting from the coordinates 44.00° N and 11.00° E, the studied area was discretized into a 1334 x 1334 grid with a grid step of 0.0015° for a detection map, while for the number of stations detecting a fixed magnitude earthquake, the grid was performed with the same step. At depth, 5 parallel planes equally spaced at 5 km were considered. A magnitude range from 0 to 1.5 with a step size of 0.1 was considered.

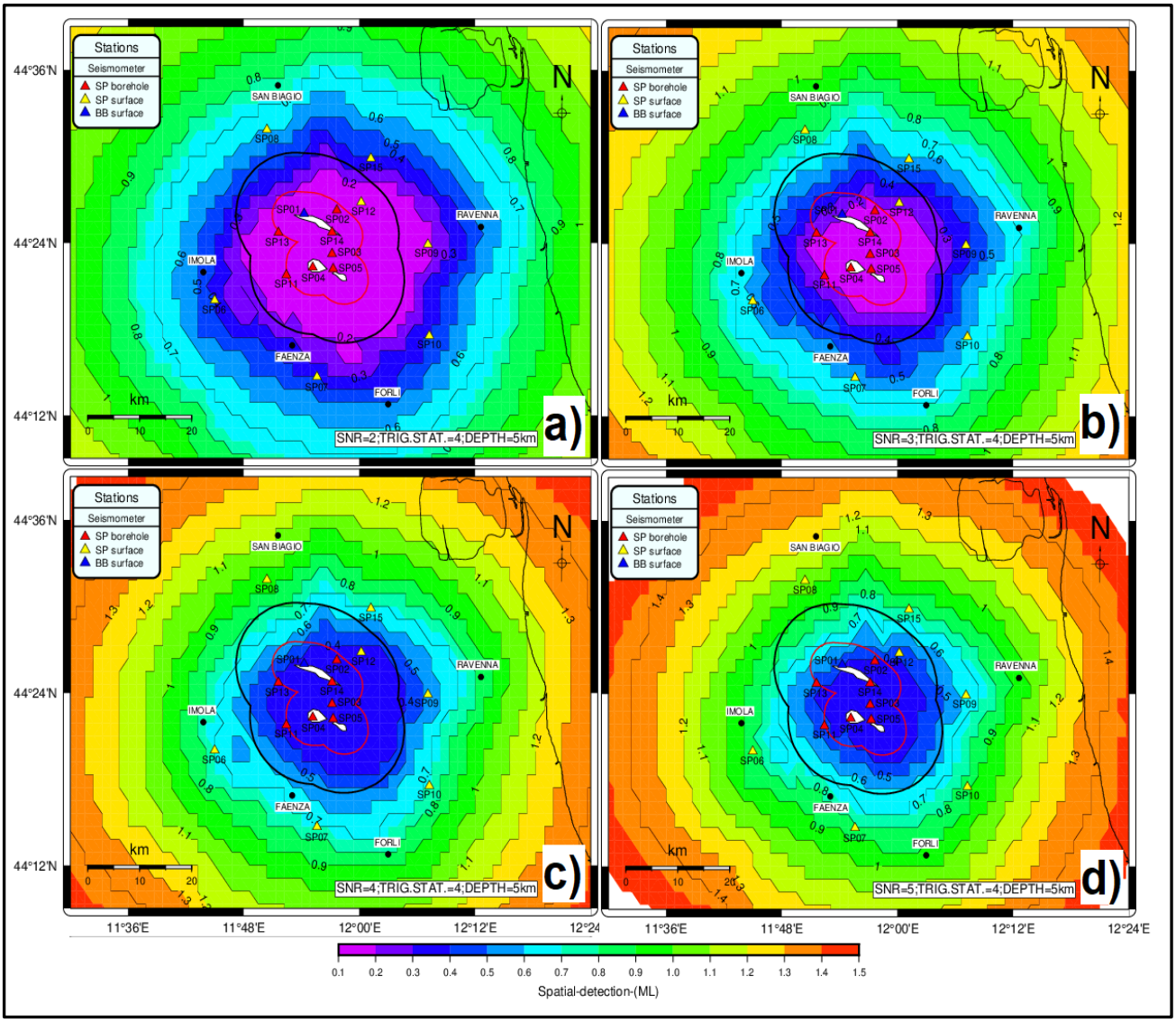

Figure 7. Detection map for the SPCMN network (see legend to identify the stations) as a function of the various parameter combinations SNR (signal-to-noise ratio) and thrsDet (number of stations to explain the detection). The magnitude contour line is defined on a grid with a grid step of 0.0015°, the depth is fixed at 5 km.

Four different SNR thresholds were tested (2, 3, 4 and 5), with the number of triggering states set to 4. For the extraction of the average seismic noise level of each station with PQLX, the "mode" between 5 and 12 Hz was selected.

The results are shown in Figure 7. Panel a) shows the detection map with SNR=2 and a minimum number of stations for a detection of 4, the overall detection capability of the network under very tolerant conditions and based on the Bragato-Trento magnitude calculation formula (used in daily routine operations). It can be seen that the network should be able to detect earthquakes with a minimum magnitude ML = 0.0 and up to 0.4 degrees, both for the storage area and for the inner area (DI). This is a suitable value for both real-time seismic monitoring and overall seismicity detection, but less favorable for the detection of induced microseismicity with magnitude values below 0, which is the target for which the network was designed.

The situation worsens considerably when the SNR value is changed to 3, which corresponds to the value set in some cases for the automatic detection system for P-waves in an STA/LTA window. In this case, the area in which the network can detect an earthquake with a minimum magnitude close to 0.0 is considerably reduced, although this detection capability is maintained in the storage areas and most of the internal area (Figure 7b). The minimum number of 4 stations is also a theoretical parameter (although it is also possible to locate with only one station).

This configuration is therefore the closest to the one defined in the monitoring system for automatic picking. However, a rather low value does not prevent a non-negligible number of false events from being detected.

A further change of the SNR value to 4 lowers the detection performance of the network to ML = 0.4, see Figure 7c.

Finally, Figure 7d shows the results for the case where the SNR value is set to 5, as intended for the detection of S-waves. The minimum detectable amplitude around the reservoir increases to 0.4 degrees and is within 0.9 for the entire reservoir as well as for the internal and external regions.

Furthermore, the detection was analyzed as a function of depth, showing a significant decrease in the detection level between 5 and 20 km. Figure 8 shows the results for different depth values, starting with panel a) for a depth of 5 km and successively increasing up to 20 km (from top left to bottom right). In these panels, we have set the SNR (signal-to-noise ratio) = 3 and thrsDet (number of stations to explain the detection) = 4. It can be observed that the detection capability of the network decreases rapidly from 5 to 20 km and the threshold increases to 0.8 in the whole storage and internal area (Figure 8d). This means that only weak earthquakes with epicenters within a depth range of 5 to 10 km are detected.

However, we believe that these results do not significantly affect the detection capacity of seismic microactivity according to the objective for which this monitoring network was designed.

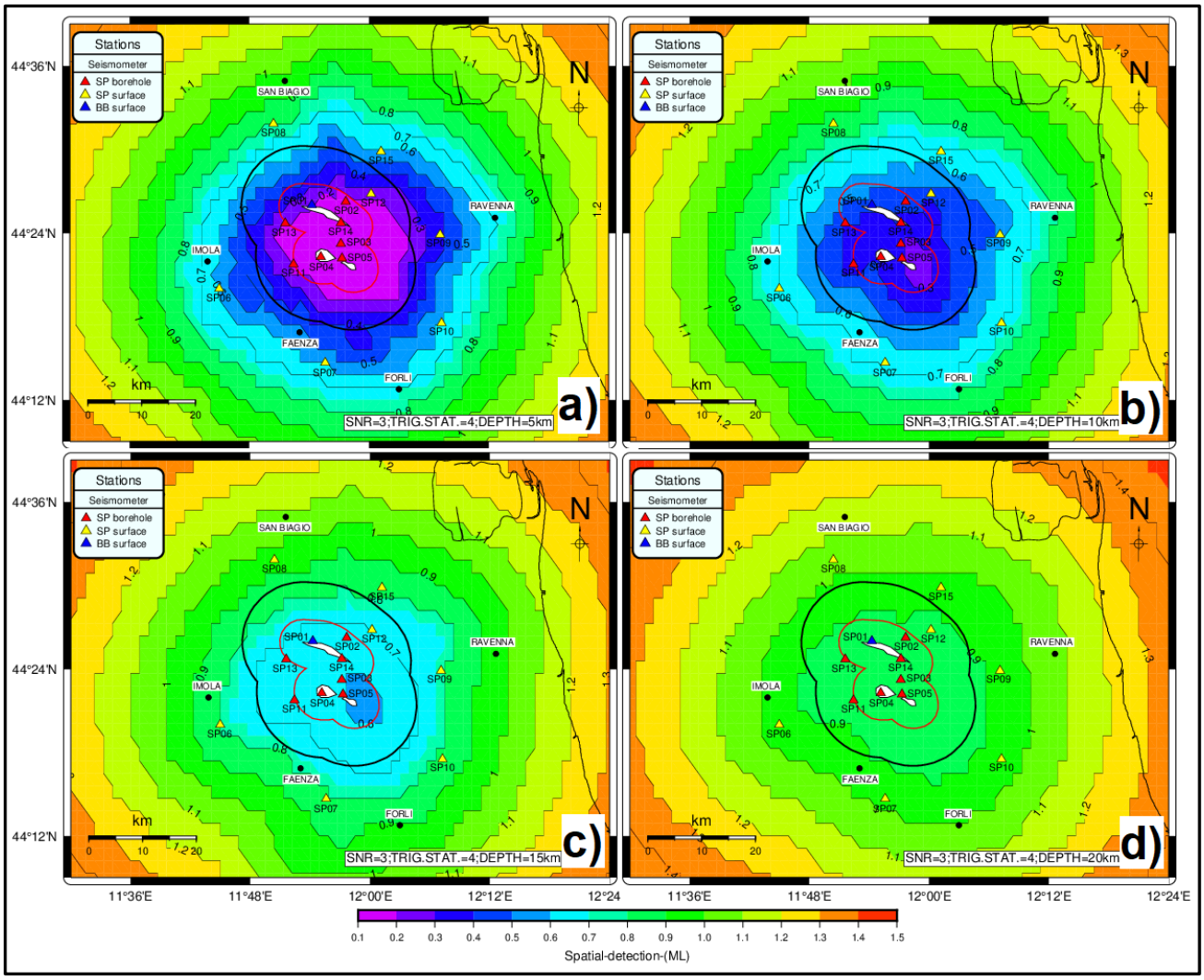

Figure 8. Detection map for the SPCMN network (see legend for identification of stations) as a function of depth and for the same parameter combination of SNR (signal-to-noise ratio) and thrsDet (number of stations to explain the detection). The magnitude contour line is defined on a grid with a grid step of 0.0015°.

Another result is the estimation of the geographical extent in which the network can detect earthquakes of a certain magnitude, based on the number of stations that fulfill the set conditions. Figure 9 shows the total number of stations that would detect a weak earthquake, again assuming the favorable condition, i.e. SNR equal to 3 and a minimum number of stations detecting the earthquake equal to 4, and determining the number of stations for different magnitude values (i.e. between 0.3 and 1.5).

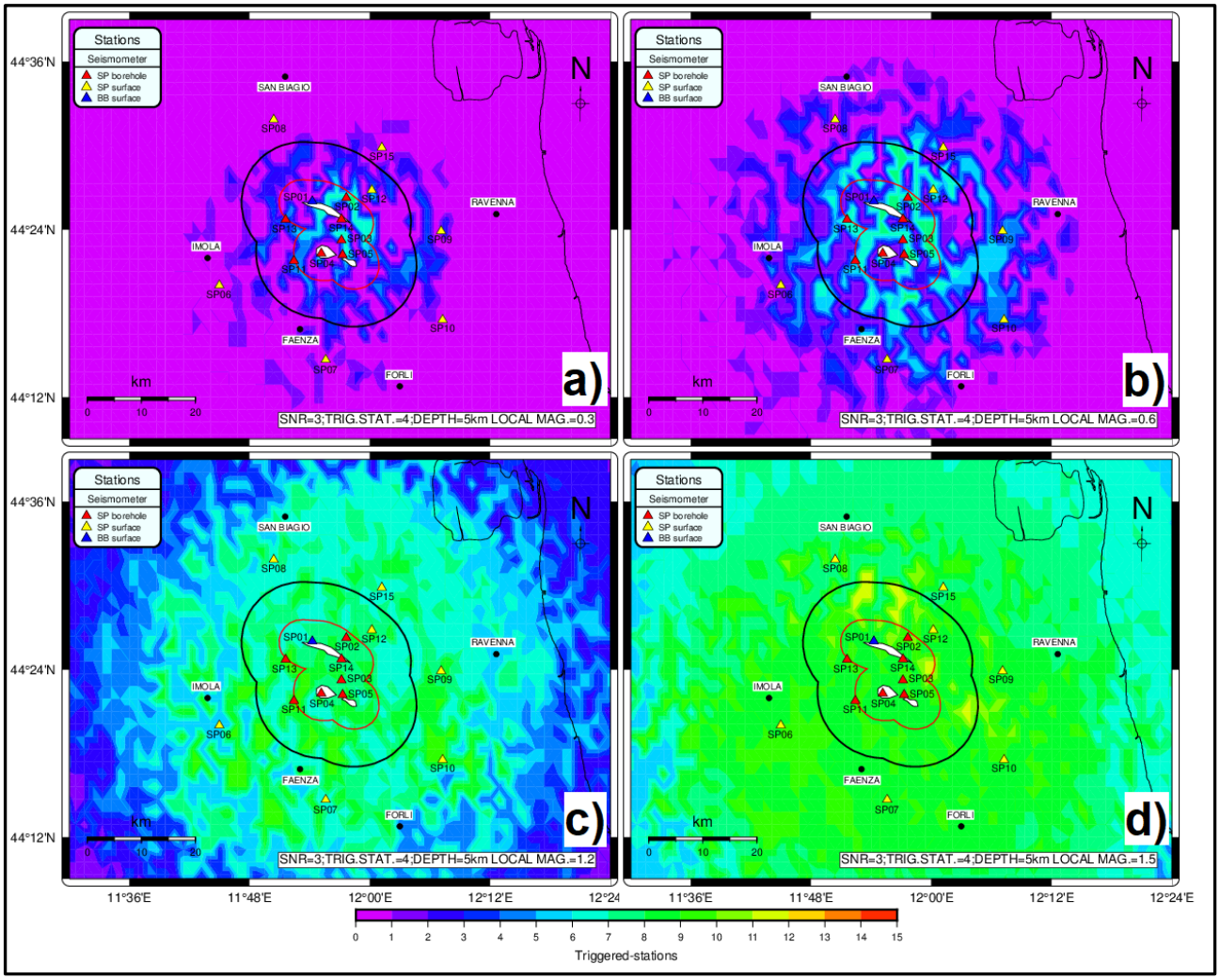

Figure 9. The station detection map for the SPCMN network (see legend for identification of stations) sets the SNR (signal-to-noise ratio) = 3 and thrsDet (number of stations to declare detection) = 4. The contour line is defined on a grid with a grid step of 0.02°, the depth is set to 5 km.

After a first analysis, we can say that the central zone of the gas reservoir and the inner area of the domain are quite well covered in terms of the number of stations that meet the detection criteria for optimal earthquake recording, which means, for example, that an earthquake of magnitude ML = 0.3 (panel a) can be detected by at least three or four stations.

For the Cotignola storage, the situation is somewhat more complicated, but improves rapidly for seismic events with ML = 0.6 and above.

It is clear that as the magnitude increases, the inner core of the network increases proportionally in terms of the number of stations that meet the conditions and that the alarm area is fully covered in terms of the functionality of all stations for events with a magnitude between ML=0.4 and ML=1.5 (Figures 9b and 9c).

Earthquakes of magnitude greater than ML=1 are detected by no less than 3 stations in the entire monitoring area.

The conclusion of this type of analysis allows us to say that the network is capable of detecting events up to ML=0.1 for almost the entire warning area, even with 33% of the stations in operation.

5. CONCLUSIONS

We have developed an analysis of the "San Potito e Cotignola" monitoring network (SPCSN) and its detection capabilities. This is the minimum value of magnitude that the network can detect at a given point in space depending on its geometry and density and the background noise level at each station, which in turn depends on the characteristics of the subsurface.

The following conclusions can be drawn from this:

- In general terms, the study area could present a number of objective difficulties, mainly related to the high degree of anthropization as well as a considerable sediment thickness in the region;
- Despite this situation, the PSD functions of the noise at the 10 stations of the network show that they are within the standards established by the Peterson NLNM and NHNM models throughout the frequency range of interest, although in some cases, e.g. at station SP01, the values approach or exceed the NHNM model;
- Background seismic noise is the factor that most affects the overall performance of the network, and the detection threshold deteriorates significantly (i.e., the minimum detection magnitude increases) the stronger the seismic noise is;
- Our study suggests that ML~ 0.1 is the minimum detectable magnitude for precisely localized earthquakes (i.e., determined by at least four stations and with SNR = 3) occurring on 100% of the reservoir area and 90% of the inner domain (ID);
- Based on the same criteria, the estimated minimum values for the detectable magnitude in the Extended Domain (ED) are between ML ~ 0.6 -1.2.
- The network is capable of detecting events with ML~ 0.1 almost for the entire alert area (including the extended domain (ED) around the storage), with the number of triggered stations at 33%.

6. Data and Resources

The "San Potito e Cotignola" monitoring network (SPCSN) is managed by Solgeo srl, www.solgeo.it. The data of the SP network are available on request from Solgeo srl, www.solgeo.it

The following software systems were used: GMT - Generic Mapping Tools (Wessel and Smith, 1991; Wessel et al., 2013; available at http://gmt.soest.hawaii.edu/; AWK (Aho et. al., 1987), with its GNU implementation GAWK; available at www.gnu.org/software/gawk; PQLX (McNamara and Boaz, 2010; available at https://www.usgs.gov/software/pqlx; and MATLAB, version 9.0.0 (R2016b), The MathWorks Inc, available at https://www.mathworks.com/products/matlab.html

7. References

Aho, A. V., B. W. Kernighan, and P. J. Weinberger (1987). The AWK Programming Language, Addison-Wesley Longman Publishing Co., Inc., Boston, MA, United States.

Aki K. & Richards P. G. 1980. Quantitative Seismology, Theory and Methods. Volume I: 557 pp., 169 illustrations. Volume II: 373 pp., 116 illustrations. ISBN 0 7167 1058 7 (Vol. I), 0 7167 1059 5 (Vol. II).

Bragato, P. L., and A. Tento (2005). Local magnitude in northeastern Italy, Bull. Seismol. Soc. Am. 95, no. 2, 579–591.

Brune, J.N. (1970). Tectonic stress and spectra of seismic shear waves from earthquake, J. Geophys. Res., 75, 4997-5009.

Cocorullo, C., Russo, L. (2018). Progettazione della rete di monitoraggio microsismico e della rete geodetica di raffittimento presso l'impianto di stoccaggio gas denominato "San Potito e Cotignola Stoccaggio" (Ra). Solgeo S.r.l. EDISON STOCCAGGIO S.p.a. ref S17MN03.

Diez, E., Sandron, D. and Guidarelli M. (2023). Evaluation of the event detection level of the "Cornegliano Laudense monitoring network". Rel. OGS 2023/58 Sez. CRS. https://hdl.handle.net/20.500.14083/22124

Diez Zaldivar, E. R., D. Sandron, and M. Cutie Mustelier (2023). Calibration of the Local Magnitude Scale (ML) for Eastern Cuba, Seismol. Res. Lett. XX, 1–13, doi: 10.1785/ 0220230286.

Diez Zaldivar, E. R., E. Priolo, D. Sandron, V. Poveda Brossard, M. Cattaneo, S. Marzorati, and R. Palau Clares (2022). Evaluation of the Event Detection Level of the Cuban Seismic Network, Seismol. Res. Lett. 93, 2048–2062, doi: 10.1785/0220220016.

Di Fronzo, F. (2018). Manuale HW rete di monitoraggio microsismico e geodetico di San Potito e Cotignola (RA). Solgeo S.r.l. EDISON STOCCAGGIO S.p.a. REF S18MN07.

Hutton, L. K. and Boore, D. M. (1987). The ML scale in Southern California. Nature, 271: 411– 414, doi:10.1038/271411a0.

IRIS (2017). Software Downloads – PQLX. Incorporated Research Institutions for Seismology, https://ds.iris.edu/ds/nodes/dmc/software/downloads/pqlx/

Marzorati, S., and M. Cattaneo (2016). Stima automatica della magnitudo minima rilevabile dalla rete sismica ReSIICO—Automatic magnitude detection of the seismic network ReSIICO, Quaderni di Geofisica 2016, Istituto Nazionale di Geofisica e Vulcanologia (INGV), 21 pp. (in Italian).

MiSE-UNMIG (2014). Indirizzi e linee guida per il monitoraggio della sismicità, delle deformazioni del suolo e delle pressioni di poro nell'ambito delle attività antropiche, 38 pp.; http://unmig.sviluppoeconomico.gov.it/unmig/agenda/upload/85_238.pdf

McNamara, D.E. and Boaz, R.I. (2005). Seismic Noise Analysis System Using Power Spectral Density Probability Density Functions: A Stand-Alone Software Package. Open-File Report 2005-1438, U.S. Department of the Interior, U.S. Geological Survey.

McNamara, D.E. and Boaz, R.I. (2010). PQLX: A seismic data quality control system description, applications, and user's manual. Open-File Report 2010-1292.

Peterson, J. (1993). Observation and modelling of seismic background noise, U.S. Geol. Surv. Open-File Rept. 93-322, 95 pp.

Sandron, D., Priolo, E. and Diez, E. (2022). The "Collalto seismic network" detection performances: some critical analysis. Rel. OGS 2022/60 Sez. CRS 5. https://hdl.handle.net/20.500.14083/17622

8. List of Figures

explain the detection). The magnitude contour line is defined on a grid with a grid step of 0.0015°, the depth is fixed at 5 km.

Figure 8. Detection map for the SPCMN network (see legend for identification of stations) as a function of depth and for the same parameter combination of SNR (signal-to-noise ratio) and thrsDet (number of stations to explain the detection). The magnitude contour line is defined on a grid with a grid step of 0.0015°.

Figure 9. The station detection map for the SPCMN network (see legend for identification of stations) sets the SNR (signal-to-noise ratio) = 3 and thrsDet (number of stations to declare detection) = 4. The contour line is defined on a grid with a grid step of 0.02°, the depth is set to 5 km.

9. APPENDIX

Appendix 1. *The noise levels of the SPCMN network stations on vertical-component broadband channel (HHZ) and short period channels (EHZ). The standard reference curves "New High Noise Model" (NHNM) and "New Low Noise Model" (NLNM) are in dark grey (Peterson, 1993).*

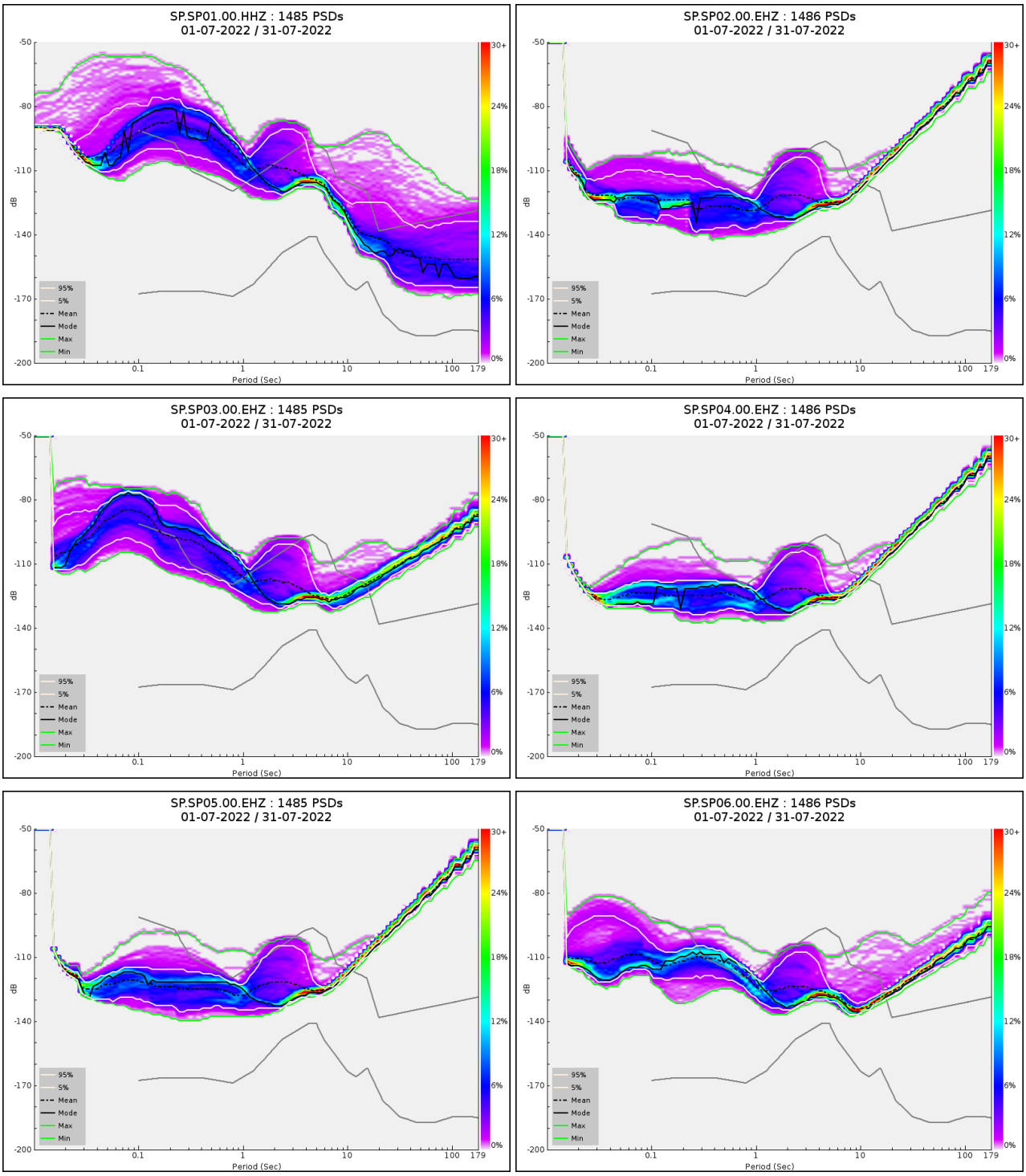

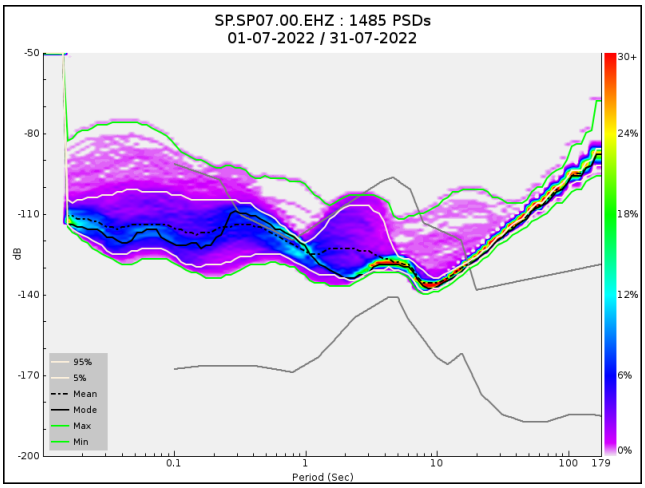
SP.SP07.00.EHZ : 1485 PSDs
01-07-2022 / 31-07-2022
dB
Period (Sec)
95%
5%
Mean
Mode
Max
Min

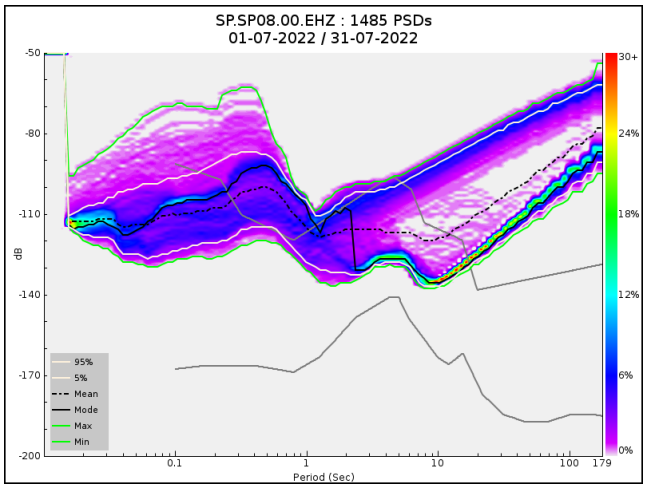
SP.SP08.00.EHZ : 1485 PSDs
01-07-2022 / 31-07-2022
dB
Period (Sec)
95%
5%
Mean
Mode
Max
Min

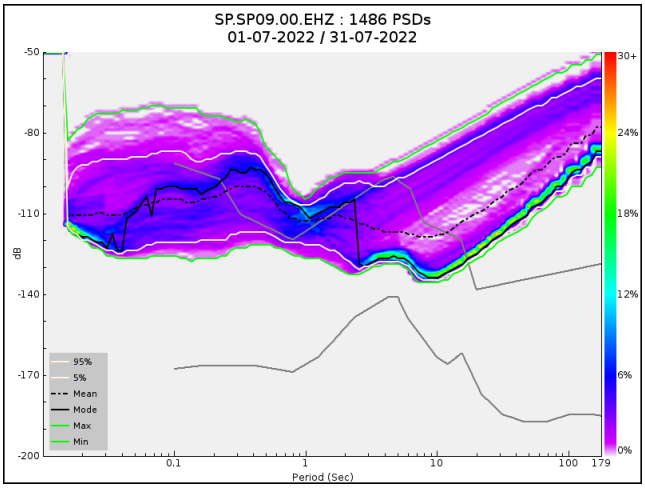
SP.SP09.00.EHZ : 1486 PSDs
01-07-2022 / 31-07-2022
dB
Period (Sec)
95%
5%
Mean
Mode
Max
Min

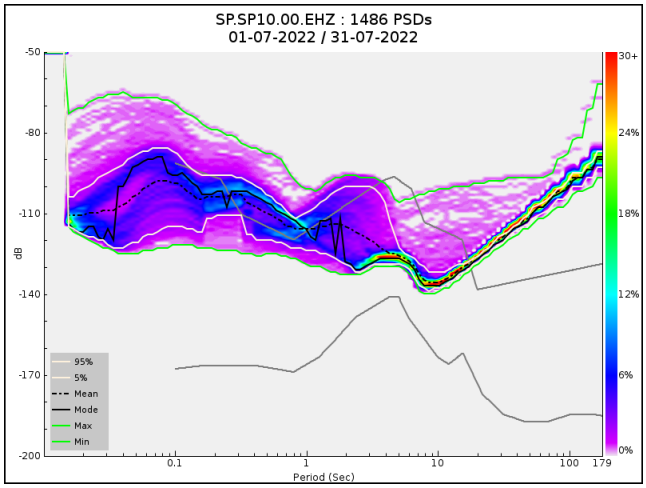
SP.SP10.00.EHZ : 1486 PSDs
01-07-2022 / 31-07-2022
dB
Period (Sec)
95%
5%
Mean
Mode
Max
Min

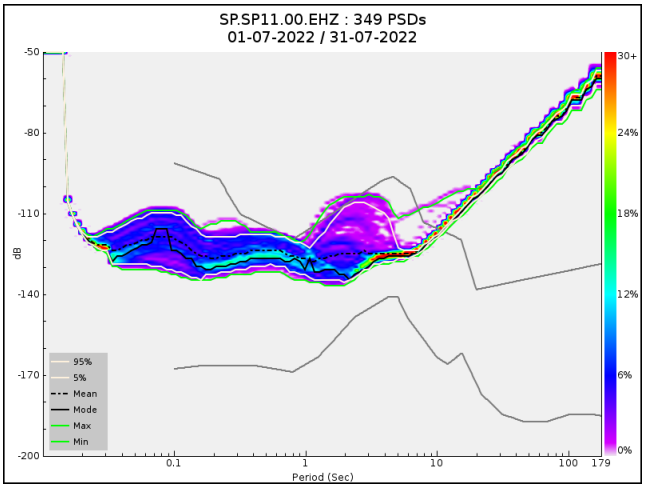
SP.SP11.00.EHZ : 349 PSDs
01-07-2022 / 31-07-2022
dB
Period (Sec)
95%
5%
Mean
Mode
Max
Min

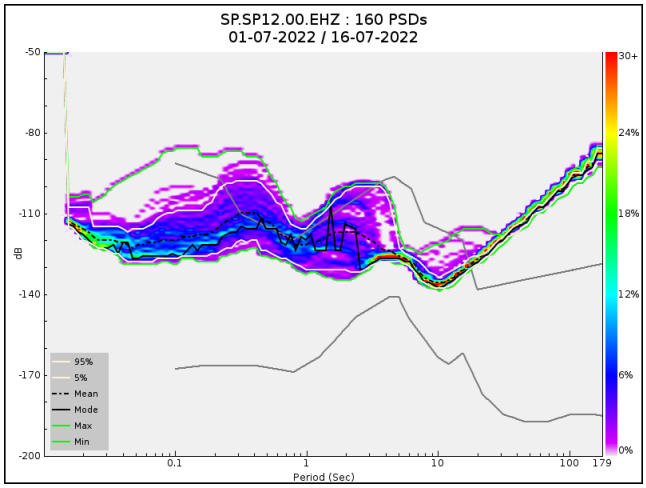
SP.SP12.00.EHZ : 160 PSDs
01-07-2022 / 16-07-2022
dB
Period (Sec)
95%
5%
Mean
Mode
Max
Min

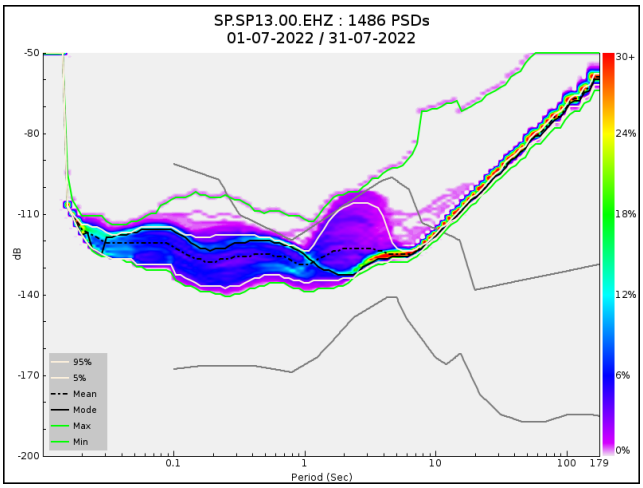
SP.SP13.00.EHZ : 1486 PSDs
01-07-2022 / 31-07-2022
dB
Period (Sec)
95%
5%
Mean
Mode
Max
Min

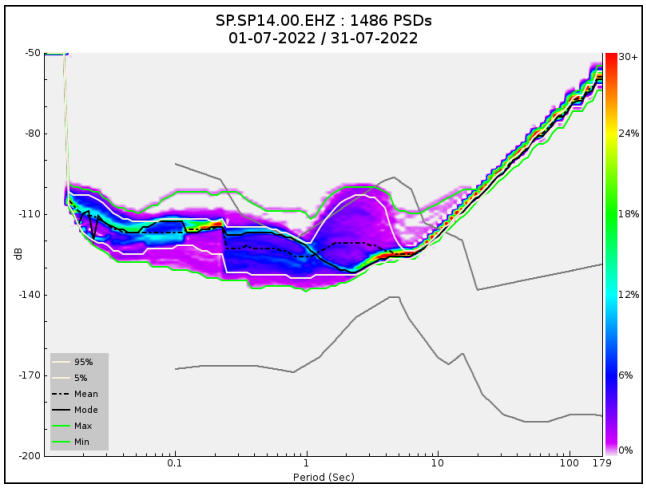
SP.SP14.00.EHZ : 1486 PSDs
01-07-2022 / 31-07-2022
dB
Period (Sec)
95%
5%
Mean
Mode
Max
Min

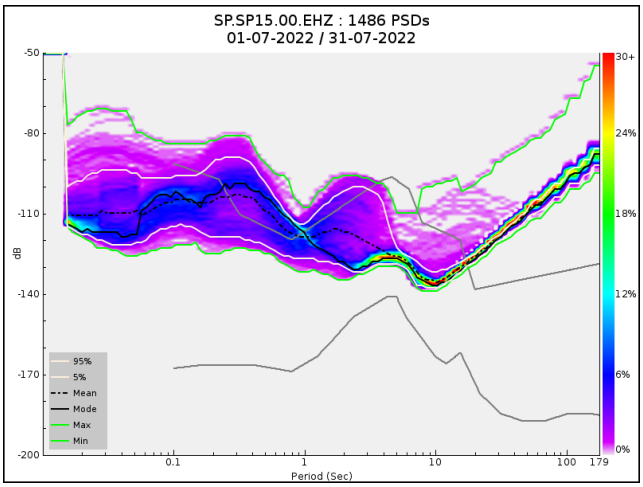
SP.SP15.00.EHZ : 1486 PSDs
01-07-2022 / 31-07-2022
dB
Period (Sec)
95%
5%
Mean
Mode
Max
Min

Appendix 2. *The transfer functions of the SP seismic network channels. a) Station SP01. Broad band sensor: SARA SS08 Digitizer: SARA SL06. b) Stations SP02,SP03, SP04, SP05, SP11, SP13, SP14 . Short period sensors: SARA SS10BH Digitizers: SOLGEO DYMAS24. c) Stations SP06,SP07, SP08, SP09, SP10, SP12, SP15 . Short period sensors: SARA SS02 Digitizers: SOLGEO DYMAS24. Source: Curves made with data kindly provided by Solgeo.*